The International Journal of Advanced Manufacturing Technology (2018) 95:4101–4116
https://doi.org/10.1007/s00170-017-1520-6

ORIGINAL ARTICLE

Investigation of hole quality during drilling of KFRP based on the interaction between collars and cutter

Sinan Liu[1] · Tao Yang[1] · Chang Liu[1] · Yu Du[1] · Wendong Gong[1]

Received: 8 August 2017 / Accepted: 18 December 2017 / Published online: 4 January 2018

Abstract
Kevlar fiber-reinforced plastic (KFRP) composites are difficult to machine and more likely to produce severe drilling-induced damage. Due to high toughness, ductile fracture of Kevlar fiber occurs after a certain extent of plastic deformation. Therefore, the mechanism of drilling-induced damages of KFRP composite cannot be accurately explained by previous damage mechanisms of carbon fiber-reinforced plastic. In this study, the mechanism of the typical drilling-induced defects of KFRP, such as delamination, tearing, and fuzzing, was systematically investigated. On this basis, a new approach (combined drilling) based on the interaction between collar (a ring-shaped device fitted on laminate) and cutter was presented to prevent damages. To investigate the effects of combined drilling on reducing drilling-induced defects, the influences of collar inner diameter and feed speed on the thrust force, delamination factor, tearing length, and fuzzing area were studied through systematic drilling experiments. Experimental results showed that delamination, tearing, and fuzzing defects were reduced with the decrease in collar inner diameter and feed speed. A reduction in defects was observed for combined drilling with collars of 6.1 mm when compared to drilling without collars at a feed rate of 20 mm/min: 26.3% for the delamination factor, 52.7% for the tearing length ratio, and 73.1% for the fuzzing area. Furthermore, a delamination model for combined drilling was proposed to predict the critical thrust force for the onset of delamination at the exit layer. Compared with experimental results, the safe limit of feed speed without causing delamination is 20 mm/min in combined drilling.

Keywords KFRP composites · Damage mechanism · Delamination · Thrust force · Hole quality

1 Introduction

Kevlar fiber-reinforced plastic (KFRP) composites, which are an important member of the family of fiber-reinforced plastics (FRPs), have been widely used in aircraft, military equipment, and body armors [1, 2]. However, due to the complicated multiphase structure, low thermal conductivity, and low interlaminar bonding strength, KFRP composites are quite difficult to drill and often cause severe machining defects [3, 4]. The severity of defects can immensely decrease machining precision, assembly accuracy, and fatigue life, which will sometimes lead to sudden failure of the composites [5]. Therefore, it is necessary to study the drilling-induced damage mechanism and investigate the approach to reduce the damage during drilling of KFRP composite laminates.

As is well-known, the most common defects are delamination, tearing, and fuzzing when drilling FRP composites [6, 7]. Hocheng et al. analyzed the mechanisms of drilling-induced delamination in carbon fiber-reinforced plastic (CFRP) laminates and concluded that the mechanisms of delamination at the entrance and the exit planes are different [8]. Delamination at the entrance is caused by the peeling force of the cutter when drilling into the laminates. During drilling to the exit, delamination occurs at some point when thrust force exceeds the interlaminar bonding strength [9]. Capello pointed out that the cutting action of the drill tip turned into punching action when the feed speed reached the threshold value, and delamination was a consequence of overload on the peripheral parts of the cutting edge [10]. Zhang et al. observed the formation process of fuzzing and tearing defects at the exit when drilling CFRP plates and assessed the exit defects [11]. Fuzzing is defined as a small number of fibers that are not cut off neatly at the edge of the hole and mainly occurs in the region where

✉ Tao Yang
yangtao@tjpu.edu.cn

[1] School of Mechanical Engineering, Tianjin Polytechnic University, Tianjin 300387, China

the angle between the fiber direction and cutting direction is acute. Tearing defect is caused by the actions of the chisel edge and the cutting edge, and the chisel edge has a primary effect on it. Since the fibers of the exit layer split from the matrix, tearing defect of drilling CFRP laminate was classified as exit delamination, and the length of tearing regions was measured to identify delamination factor [12]. To the authors' knowledge, previous literatures have mainly focused on the damage mechanism of CFRP composites. However, different characteristics of KFRP composite will result in significant discrepancies of the damage mechanism. First, the interfacial bonding between fibers and matrix of KFRP composites is lower than that of CFRP, which makes debonding of Kevlar fiber/matrix interface more likely to occur [13]. Second, carbon fiber is a brittle material with high hardness, while Kevlar fiber is a flexible material with high toughness. The failure behavior of Kevlar fibers, which fracture after a certain extent of plastic deformation, is entirely different to that of carbon fibers [14, 15]. Finally, Kevlar fibers tend to slip along the axial direction and split during machining, and the fracture morphology exhibits formation of fibrils within the individual fibers [16]. Therefore, the mechanism of drilling-induced damages of KFRP composites cannot be accurately described by the current literatures relating to CFRPs. Until now, no systematic study on mechanisms of drilling-induced damages of KFRP composites (delamination, tearing, and fuzzing) has been performed, whereas it is essential for a better understanding.

Researchers have investigated the phenomena of manufacturing defects during drilling of FRP laminates [17–20]. The approach of using backup plates is the most widely used. Tsao et al. proposed models of critical thrust force to analyze the effects of saw drill and core drill on CFRP laminates with backup plates. Results showed that critical thrust force could be improved significantly to prevent delamination defect at the exit [21]. Using finite-element analysis, Bhattacharyya et al. concluded that direct stresses were compressive and low, and any major surface delamination in mode I was unlikely to happen when drilling KFRP composite with a back support [3]. However, there are still some disadvantages of the approach. Firstly, due to abrasive and cohesive action, severe tool wear occurs during drilling of FRP laminates [18, 22]. In addition, tool wear is aggravated when the drill enters into sacrificial plates, which are usually made of aluminum or some other hard material of high density. Secondly, under the drilling action, chip of sacrificial plates repeatedly scrapes the machining surface and the interface between laminate and plates, and a portion of chip is mixed in the damage areas. Therefore, this study presents a new approach of drilling and systematically investigates the internal mechanism to inhibit the damage during drilling of KFRP composites. As illustrated in Fig. 1, a pair of collars is fixed at the entrance and the exit planes. The upper collar compresses the laminate, and the under collar supports it. The cutter moves across the hole of the collars to avoid tool wear. Drilling of the laminate is initiated under the interaction between collars and cutter and is referred to as combined drilling. The major advantages of combined drilling can be summarized as follows. Firstly, combined shearing action between the cutting edge and the edge of the hole-wall of the collar facilitates cutting of Kevlar fibers and restrains fuzzing and tearing defects. Secondly, compressive force F_1 exerted by the upper collar and supporting force F_2 exerted by the under collar increase the stiffness of the process system, thus inhibiting delamination propagation.

The remainder of this paper is organized as follows. In Sect. 2, drilling experiments of KFRP composites were presented, and mechanical property tests were conducted to obtain material properties of laminates. In Sect. 3, damage mechanism and corresponding inhibition mechanism were analyzed systematically. Section 4 introduced the delamination model to predict critical thrust force for the onset of delamination at the exit. Moreover, the influence of feed speed and supporting configuration on the distribution of maximum thrust force was discussed deeply. In Sect. 5, delamination factor, tearing length ratio, and fuzzing area were introduced

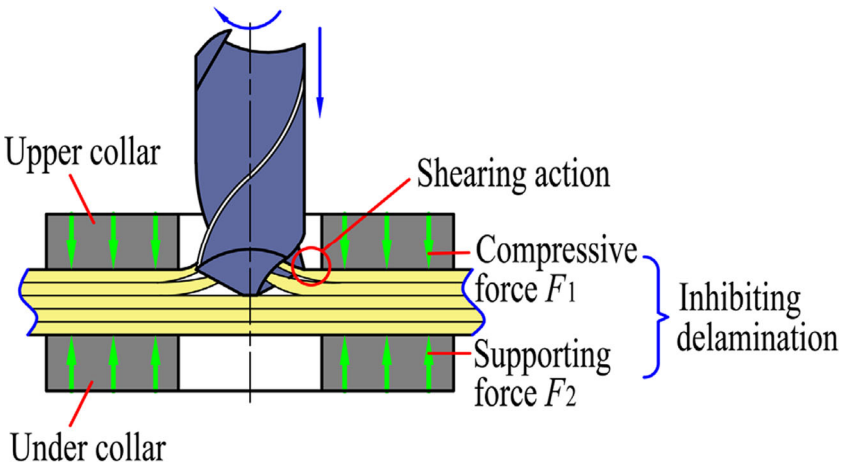

Fig. 1 Schematic diagram of combined drilling

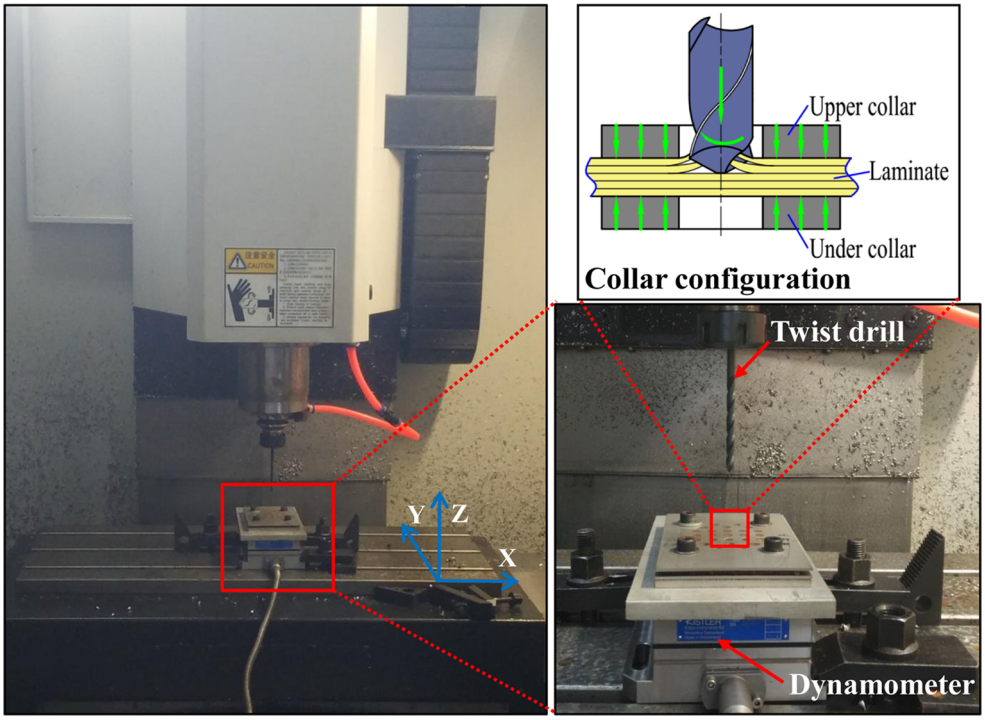

Fig. 2 Experimental devices of drilling

to quantitatively characterize the hole quality. Experimental results showed that machining defects were reduced effectively. Some useful conclusions were drawn in Sect. 6.

2 Experimentation

2.1 Material preparation

The KFRP composite laminates were produced using plain weave prepregs. The volume fraction of phenolic resin matrix was 38%. The laminates with 13 plies were cured by autoclaving at 110 °C for 60 min followed by 180 °C for 120 min. After cooling, laminates were cut into specimens of 150 mm × 95 mm with a 3.5-mm thickness for drilling; the thickness of each layer was 3.5/13 ≈ 0.27 mm.

2.2 Drilling experiment setup

To study the drilling-induced damage mechanism of KFRP, experiments were carried out on a CNC vertical milling machine (XK714D, Hanland). As shown in Fig. 2, the standard

Table 1 Drilling parameters for testing and experimental values of thrust force

Working condition	Test number	Size of collar c (mm)	Feed speed f (mm/min)	F_{max} (N)	F_{last} (N)
A_1	1	Without	20	43.7	26.0
A_1	2	Without	40	59.5	39.9
A_1	3	Without	80	64.8	54.9
A_2	4	6.1	20	58.0	31.9
A_2	5	6.1	40	70.4	48.9
A_2	6	6.1	80	81.6	55.8
A_3	7	6.3	20	53.2	29.9
A_3	8	6.3	40	62.5	48.2
A_3	9	6.3	80	72.1	50.2
A_4	10	6.5	20	49.5	27.3
A_4	11	6.5	40	57.3	43.1
A_4	12	6.5	80	60.4	42.6
A_5	13	6.7	20	43.7	28.2
A_5	14	6.7	40	51.0	40.6
A_5	15	6.7	80	55.2	45.0

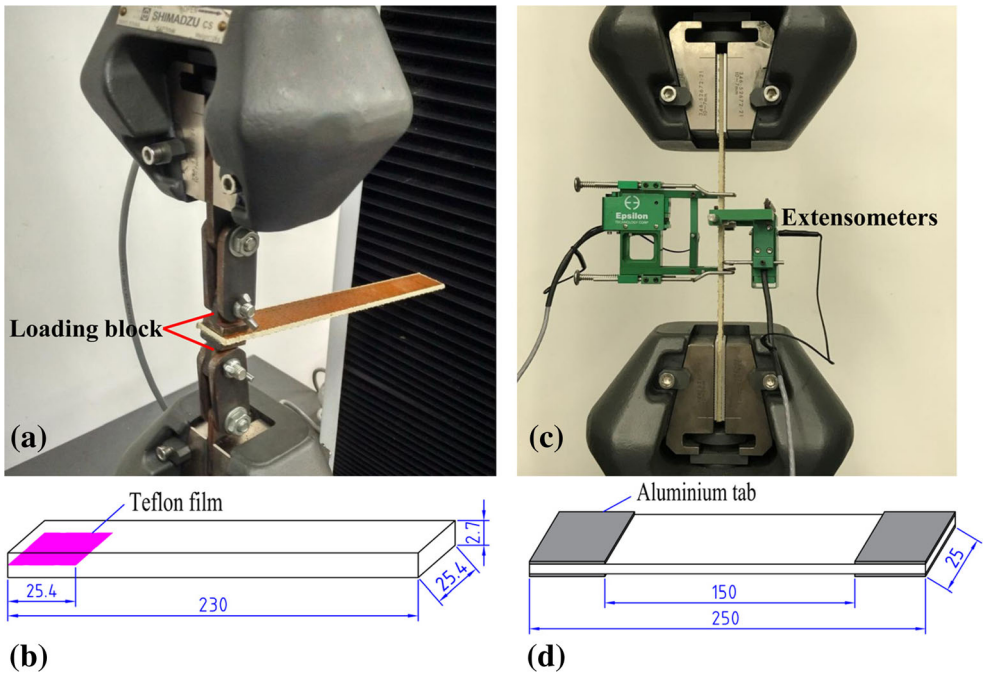

Fig. 3 Experimental setup of mechanical property test

HSS twist drills with a point angle of 118° and diameter of 6 mm were used. To simulate the collar configuration in combined drilling, a pair of 2-mm-thick stainless steel plates with prefabricated holes was fixed on the upper and the lower surfaces of the laminate. A dynamometer (9257B, Kistler) was connected to a charge amplifier (5070A, Kistler) and mounted on the machining table to measure the dynamic cutting force.

In order to prevent cutting the collars, the inner diameter of collar should be slightly larger than the diameter of the twist drill. Therefore, the inner diameters of collars were selected as 6.1, 6.3, 6.5, and 6.7 mm. The feed speed was determined as 20, 40, and 80 mm/min. Since cutting speed has a less influence on hole quality [23], the cutting speed was set to 62.8 m/min. In order to analyze the influence of drilling parameters on hole quality, a single variable was varied in each group of drilling tests. The corresponding drilling parameters and experimental values of thrust force are listed in Table 1. Drilling without plates will subsequently be referred to as working condition A_1, and combined drilling is referred to as working condition A_2–A_5. Owing to the hygroscopicity of KFRP composites, the experiments were conducted in dry cutting. Because the chip and dust generated during drilling can cause damage to people's respiratory system, experimenters should wear masks.

2.3 Mechanical properties of KFRP laminate

Mechanical property tests were conducted to obtain material properties of the KFRP laminate. The measured properties were then used to predict the critical thrust force for the onset of delamination. As shown in Fig. 3a, the interlaminar fracture toughness in mode I was measured in the double cantilever beam (DCB) test. The test was executed on a universal testing machine (AGS-X-50KND, Shimadzu) at a constant loading speed of 1.27 mm/min. A pair of loading blocks was attached to the specimen using two-component epoxy adhesive. Dimensions of the specimen used in the DCB test are shown in Fig. 3b. The initial crack was prefabricated with a Teflon film in the midplane of the laminate. The length and thickness of the film were 25.4 mm and 20 μm, respectively. The crack was marked at 10-mm intervals from the tip of the Teflon film.

The interlaminar fracture toughness in mode I can be calculated by

$$G_{\mathrm{I}} = \frac{3P_{\mathrm{c}}\delta_{\mathrm{c}}}{2ba} \tag{1}$$

where P_{c} is the applied tensile load to produce stable crack growth, δ_{c} is the crosshead displacement, b is the width of the specimen, and a is the crack length.

When the crack grew to the first mark, we stopped the loading and the crosshead displacement δ_{c} and the corresponding load P_{c} were measured. Then, we repeated the process until the crosshead displacement reached approximately 30% of the crack length, and values were recorded at each interval.

Table 2 Properties of KFRP composites

Mode I fracture toughness G_{IC} (J/m^2)	Tensile modulus E (GPa)	Poisson's ratio
202.37	6.1	0.29

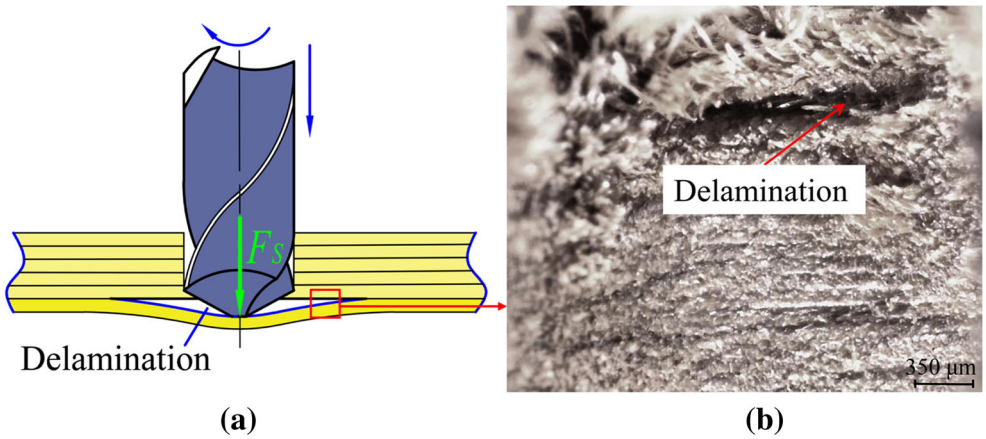

Fig. 4 **a** Schematic diagram of delamination mechanism. **b** Delamination defect during drilling of KFRP

Tensile modulus and Poisson's ratio were also measured in the tensile test. As shown in Fig. 3c, Epsilon extensometers were installed on the specimen. The tensile force was applied at a loading rate of 2 mm/min. Dimensions of the specimen used in the tensile test are shown in Fig. 3d. Using two-component epoxy adhesive, aluminum tabs of 2-mm thickness were adhered to the ends of the specimen. Based on above tests, the mechanical properties of KFRP laminate can be obtained as listed in Table 2.

3 Damage mechanisms and inhibition mechanisms of KFRP composites

3.1 Delamination

The schematic diagram of delamination is illustrated in Fig. 4a. When drilling toward the exit, the thickness of uncut layers is decreased, and elastic deformation occurs due to the thrust force applied by drill. At some point, delamination will occur when thrust force exceeds the interlaminar bonding strength. In addition, due to low interfacial bonding between Kevlar fibers and matrix, delamination of drilling KFRP composites is more pronounced. Through a digital microscope (DVM6, Leica), a delamination defect close to the exit is shown in Fig. 4b.

In order to avoid delamination, thrust force exerted by drill should not exceed the critical value. Based on linear elastic fracture mechanics (LEFM) and theory of classic plate bending, the critical thrust force can be calculated through delamination model. The delamination model considering the interaction between collar and cutter will be analyzed later (Sect. 4.1) to predict the critical thrust force at the onset of delamination in combined drilling of KFRP composite.

3.2 Tearing

As shown in Fig. 5a, tearing damage is initiated in the process: The exit layer splits around the drill point under the punching action of the chisel edge. The majority of fibers are failed by tensile failure due to the high toughness. This effect is mainly caused by the negative rake angle of the chisel edge. Since there is no effective support at the exit, Kevlar fibers are bended and twisted under the thrust force and the torque of the cutting edge. Consequently, the tearing damage extends further after the chisel edge penetration. As shown in Fig. 5b, Kevlar fibers slip along the axial direction and split after machining, such that severe tearing defect occurs along the edge of the hole.

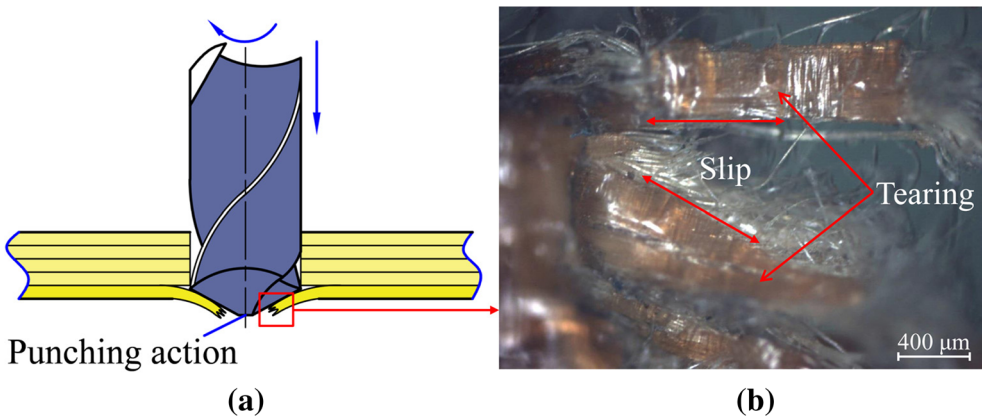

Fig. 5 **a** Schematic diagram of tearing mechanism. **b** Tearing defect during drilling of KFRP

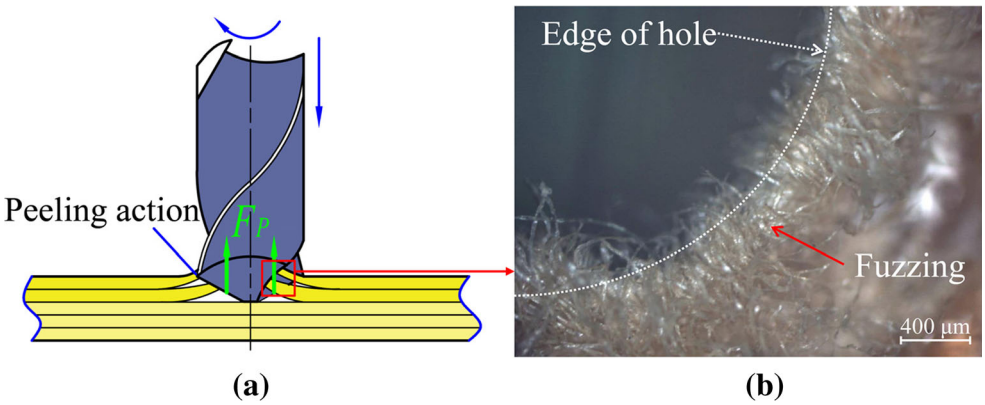

Fig. 6 **a** Schematic diagram of fuzzing mechanism. **b** Fuzzing defect during drilling of KFRP

3.3 Fuzzing

The schematic diagram of fuzzing mechanism is shown in Fig. 6a. As shown in Fig. 6b, fuzzing defect appears flocculent and stacking along the edge of hole. Because the entrance plane is a free surface, uncut material is torn and pulled by the drill flute under the peeling force F_P exerted by the drill. During this process, few fibers are failed by shear failure. In contrast, due to the high toughness of Kevlar fiber, obvious yielding and necking are caused by the peeling action, such that Kevlar fiber fractures after a certain extent of plastic deformation. Therefore, the fracture of Kevlar fiber is uneven and characterized by ductile fracture.

3.4 Inhibiting drilling-induced damages

The schematic diagram of inhibiting tearing defect is presented in Fig. 7. During combined drilling of KFRP composites, the drill cuts the laminate under the interaction between collars and cutter. The collar clamps the exit plane; thus, Kevlar fibers bear tensile stress, which restrains bending deformation and conceding to some extent. In the drilling process, Kevlar fibers are moved under the action of the revolving cutting edge. Meanwhile, there is also relative motion between Kevlar fibers and static edge of the hole-wall of the collar, such that fiber layers are subjected to shear forces from the cutting edge and edge of the hole-wall of the collar simultaneously. Therefore, shear fracture is strengthened to reduce tearing defect. Moreover, extension of tearing defect to non-machining region can be prevented by supporting force F_2.

Figure 8 illustrates the schematic diagram of inhibiting fuzzing defect. Since the collar clamps the ends of the material at the entrance plane, Kevlar fibers bear tensile stress. Consequently, the sliding and spring back of fibers are restrained. During the motion of cutting edge along the edge of the hole-wall of the collar, shear fracture is strengthened because of combined shearing action exerted from the collar and cutter. Therefore, tensile failure of Kevlar fiber is restrained, and hole quality at the entrance is improved effectively. In addition, the extension of fuzzing defect to non-machining region can be prevented by compressive force F_1, exerted by the upper collar.

4 Thrust force

4.1 Delamination model

In order to model the critical thrust force for the onset of delamination, the classic plate bending theory of a circular plate with the ends clamped is introduced. Moreover, the mechanical properties are the same in the transverse and longitudinal directions for the plain-weave KFRP composite. Therefore, it is assumed that the circular plate is isotropic in

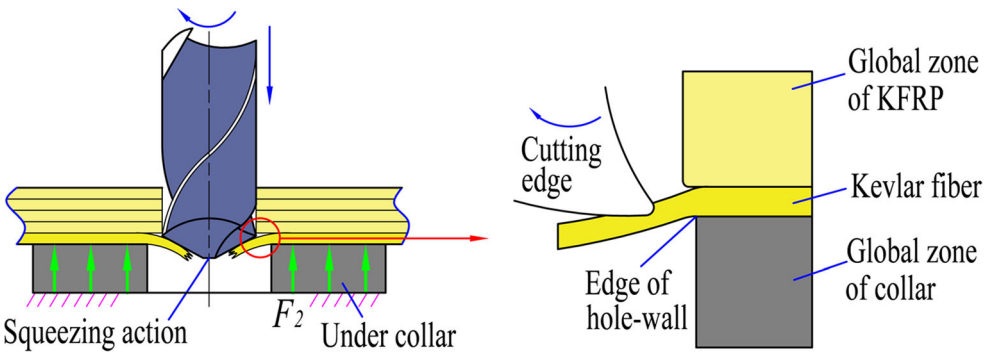

Fig. 7 Schematic diagram of inhibiting tearing defect

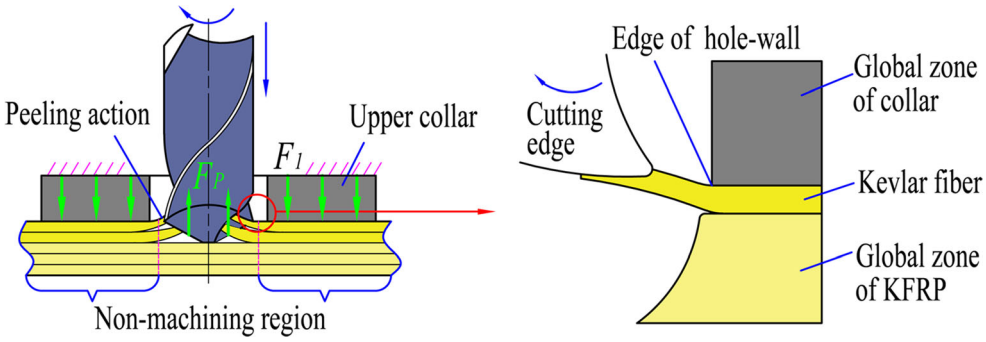

Fig. 8 Schematic diagram of inhibiting fuzzing defect

this model. The energy balance equation from LEFM can be written as [8]

$$G_{IC}\mathrm{d}A = F_S\mathrm{d}Z - \mathrm{d}U \tag{2}$$

where G_{IC} is the interlaminar fracture toughness in mode I, dA is the increment of the area of delamination crack, F_S is the compressive thrust force, dZ is the differential of drill movement, and dU is the infinitesimal strain energy.

Figure 9 demonstrates the delamination mechanism at the exit in combined drilling. Due to the compressive thrust force, elastic deformation of the uncut lamina occurs, and the delamination crack is initiated. As the chisel edge pushes down, the delamination crack propagates further and exceeds the span of the inner hole of the collar. Due to the supporting force of the collar, the surrounding region of the uncut layer is lifted slightly. Because the stiffness of the collar is much higher than the stiffness of the uncut layer, the surface contact between the collar and the laminate turns to a line contact along the periphery of the inner hole. As a result, the supporting force changes to a circular load. In this model, c is the radius of the inner hole of collar, a is the assumed size of the crack, h is the thickness of the uncut lamina, and the circular load of the radius c is defined as q.

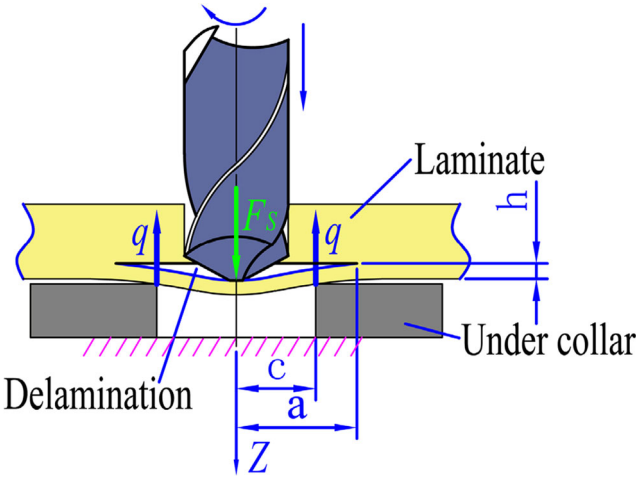

Fig. 9 Schematic diagram of delamination model in combined drilling

The deformed lamina is subjected to thrust force F_S and supporting circular load q. Therefore, the energy balance equation in this model can be expressed as

$$G_{IC}\mathrm{d}A = \left(F_S\mathrm{d}Z_1 - \mathrm{d}U_1\right) - \left(2\pi cq\mathrm{d}Z_2 - \mathrm{d}U_2\right) \tag{3}$$

where subscripts 1 and 2 denote the variables of thrust force F_S and q, respectively. The directions of Z_1 and Z_2 are opposite. It can be seen from Eq. 3 that four variables, Z_1, Z_2, U_1, and U_2, need to be calculated. The detailed explanations are given as follows.

The deflection and the strain energy of a circular plate under the action of thrust force are given as [8]

$$Z_1 = \frac{F_S a^2}{16\pi D} \tag{4}$$

$$U_1 = \frac{8\pi D Z^2}{a^2} \tag{5}$$

The flexural rigidity D expressed as follows is related with the elastic modulus E and the Poisson ratio υ:

$$D = \frac{Eh^3}{12(1-\upsilon^2)} \tag{6}$$

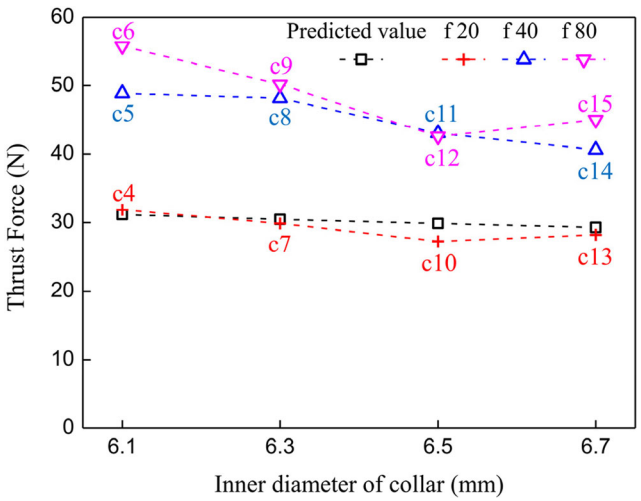

Fig. 10 Comparison of measured and predicted thrust forces of the last ply in combined drilling

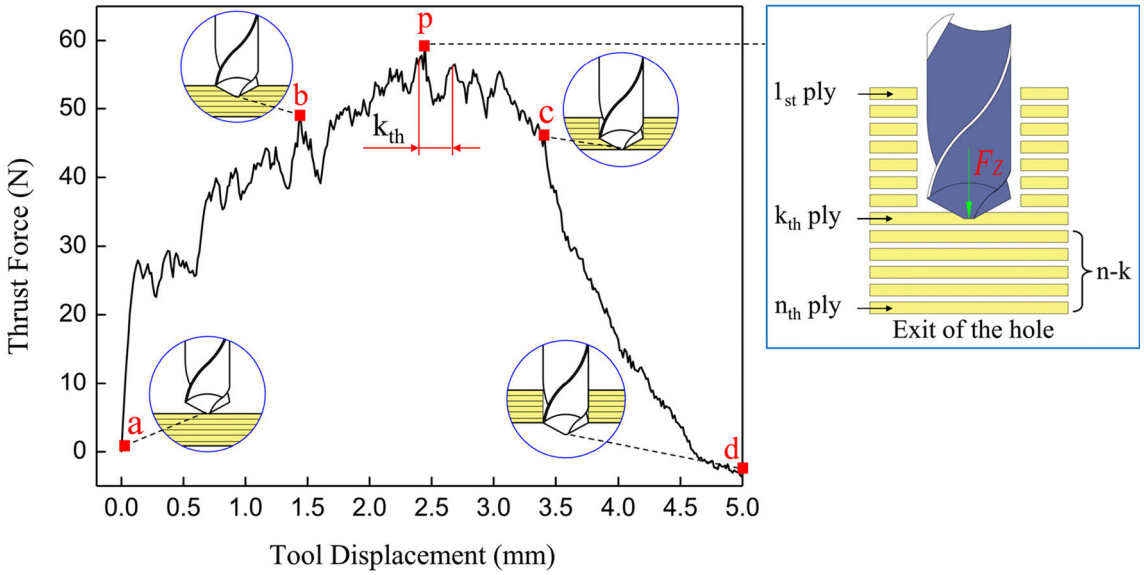

Fig. 11 Thrust force curve over one drilling cycle

The inner and outer deflections under the circular load can be calculated by [21]

when $0 \le r \le c$

$$Z_{2IN} = \frac{2\pi cq}{8\pi D}\left[\left(a^2 - r^2\right)\frac{a^2 + c^2}{2a^2} + \left(c^2 + r^2\right)\ln\frac{r}{a}\right] \tag{7}$$

when $c < r \le a$

$$Z_{2OUT} = \frac{2\pi cq}{8\pi D}\left[\left(c^2 + r^2\right)\ln\frac{c}{a} + \frac{\left(a^2 - c^2\right)\left(a^2 + r^2\right)}{2a^2}\right] \tag{8}$$

The strain energy under the action of circular load can be calculated as follows:

$$U_2 = \pi D\left(\begin{array}{l}\int_0^c \left(\frac{\mathrm{d}^2 Z_{2IN}}{\mathrm{d}r^2} + \frac{1}{r}\frac{\mathrm{d}Z_{2IN}}{\mathrm{d}r}\right)^2 r\mathrm{d}r \\ + \int_c^a \left(\frac{\mathrm{d}^2 Z_{2OUT}}{\mathrm{d}r^2} + \frac{1}{r}\frac{\mathrm{d}Z_{2OUT}}{\mathrm{d}r}\right)^2 r\mathrm{d}r\end{array}\right) \tag{9}$$

In addition, the supporting circular load of the collar is equal to the compressive thrust force of the cutter. Consequently, this is an implicit equation, $F_S = 2\pi cq$. Let $s = c/a$ and substitute Eqs. 4, 5, and 7–9 into Eq. 3, and the critical thrust force at the onset of crack propagation in combined drilling can be finally calculated as

$$F_S = \frac{\pi}{s}\sqrt{\frac{8G_{IC}Eh^3}{3(2-s^2)(1-\upsilon^2)}} \tag{10}$$

Figure 10 represents the comparison of the measured thrust force and the predicted values of the last ply in different working conditions. The numerals indicate the test numbers in Table 1, and the letter "c" represents the chisel edge breaking through the last ply of the laminate. It can be observed that the predicted force for the onset of delamination agrees well with the experimental measurements at a feed speed of 20 mm/min. The trend of the predicted force is consistent with the experimental measurements, wherein the thrust force declined when the inner diameter of collars increased. Moreover, the measurements were higher than the predicted values at feed speeds of 40 and 80 mm/min. It can be concluded that the safe limit of feed speed is 20 mm/min to avoid delamination in combined drilling.

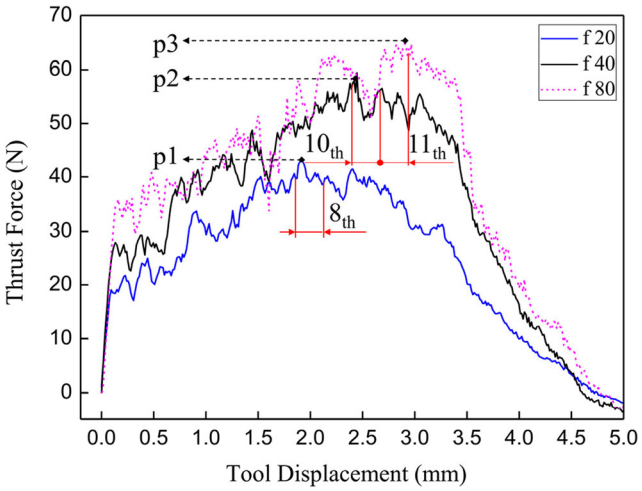

Fig. 12 Distribution of the maximum thrust force of working condition A_1

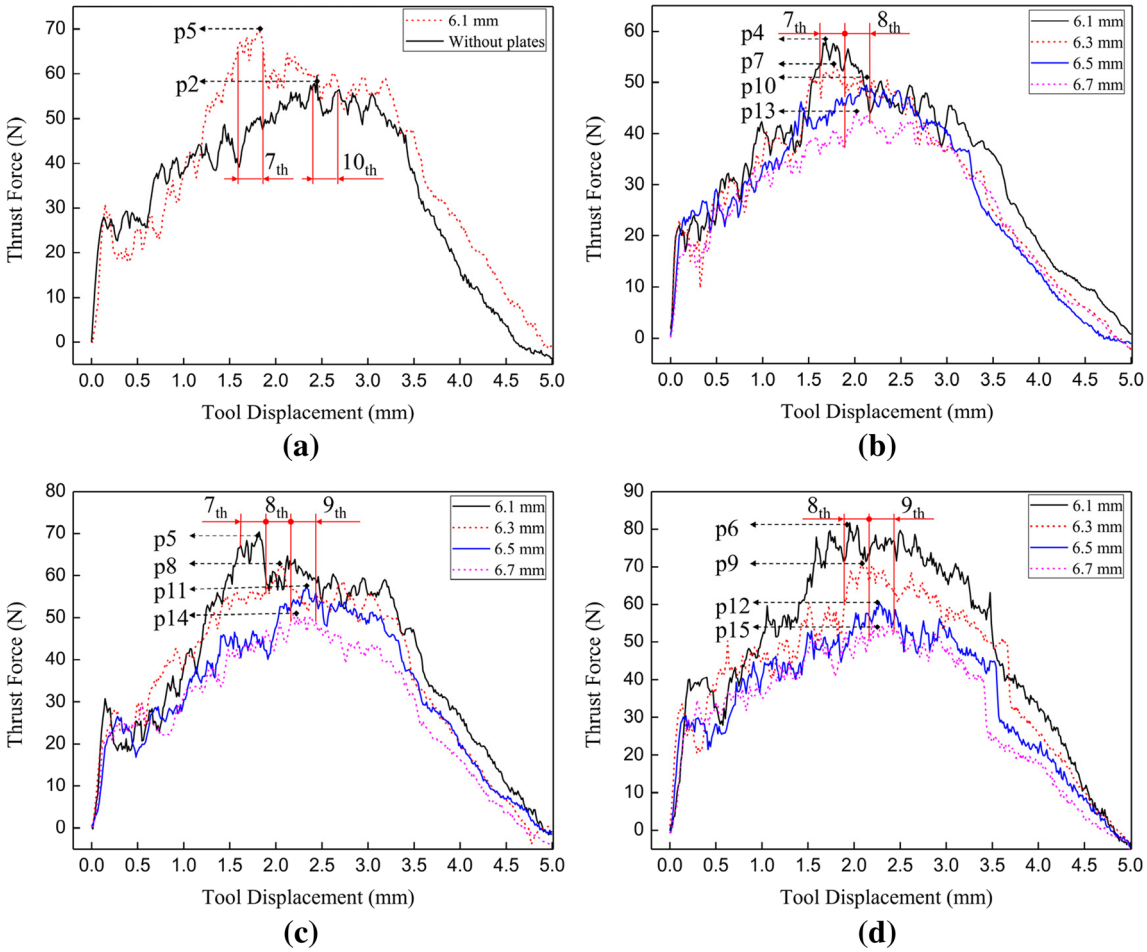

Fig. 13 Distribution of the maximum thrust force of combined drilling. **a** 6.1 mm vs. without plates. **b** $f = 20$ mm/min. **c** $f = 40$ mm/min. **d** $f = 80$ mm/min

4.2 Distribution of the maximum thrust force

4.2.1 Drilling without plates

Cured resin matrix is known as a brittle material, while Kevlar fiber is a flexible material with high toughness. Therefore, the failure behavior of Kevlar fiber is quite different from that of resin matrix. During the process of drilling KFRP composites, the cutting edge cuts the Kevlar fibers and resin matrix alternately. Therefore, this process causes the thrust force to fluctuate significantly. Figure 11 illustrates the typical thrust force curve over one drilling cycle of KFRP composites. Five key nodes (a, b, p, c, and d) are shown on the curve. At the beginning of drilling process, thrust force rises rapidly when the drill enters into the laminate (point a). Then, the whole main cutting edge is involved in machining (point b) until the chisel edge breaks through the last ply of the laminate (point c). During the whole drilling period, thrust force fluctuates significantly and increases to the maximum value (point p) when the drill point enters into the kth ply (i.e., the number of uncut plies under drill point is $n - k$). When the whole main cutting edge penetrates the laminate (point d), thrust force decreases to 0.

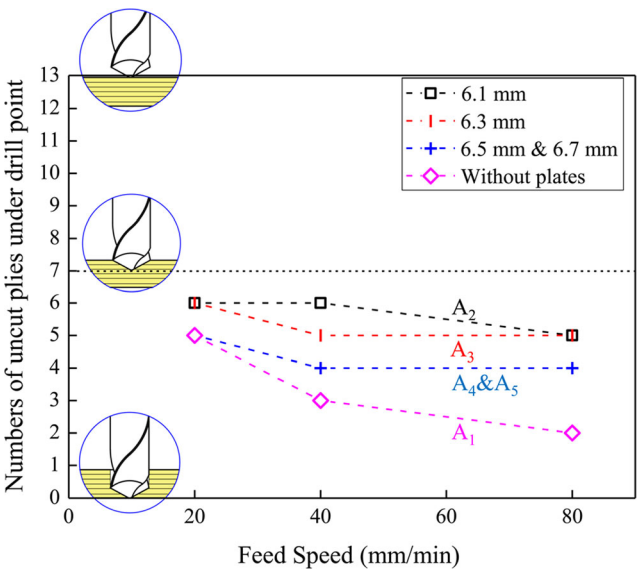

Fig. 14 Position of drill point at maximum thrust force

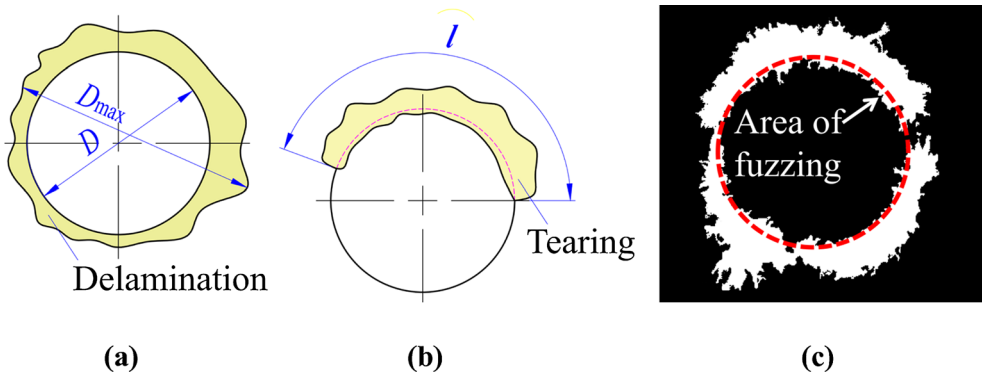

Fig. 15 Characterization of hole quality. **a** Delamination defect. **b** Tearing defect. **c** Fuzzing defect

Comparison of thrust force curves of working condition A_1 is shown in Fig. 12. It can be observed that with a feed speed of 80 mm/min, thrust force reaches the maximum value of 64.8 N (point p3) when the drill point enters into the 11th ply. Moreover, the position of the drill point is close to the last ply of the laminate (13th ply). Reducing the feed speed to 20 mm/min, thrust force reaches the maximum value of 43.7 N (point p1) when the drill point enters into the eighth ply. In addition, the position of the drill point is close to the point at which the whole main cutting edge enters into the laminate (sixth ply). Therefore, feed speed has a large influence on the distribution of the maximum thrust force. When feed speed decreases from 80 to 20 mm/min, the position of the maximum thrust force moves toward the ply at which the whole main cutting edge enters into the laminate. The main reason for this phenomenon is that the temperature of drill point rises in proportion to the square root of machining time [24]. The machining time of $f = 20$ mm/min is double that of $f = 40$ mm/min and quadruple that of $f = 80$ mm/min. The lower the feed speed is, the higher the drill point temperature rises. In the case of $f = 20$ mm/min, after the whole main cutting edge entering into the sixth ply, the matrix is softened by heat accumulating around the cutting edge. Therefore, the stiffness coefficient decreases [25, 26], and thrust force declines gradually from drilling to the eighth ply.

4.2.2 Combined drilling

Figure 13a shows the comparison of thrust force curves during drilling with collar of 6.1 mm and without plates in the case of $f = 40$ mm/min. The red dotted line is the thrust force curve with collar of 6.1 mm, and the black solid line is the thrust force curve without plate. During drilling without plates, the thrust force reaches to the maximum of 59.5 N (point p2) when the drill point enters into the tenth ply. During drilling with collars of 6.1 mm, thrust force rises to the maximum of 70.4 N (point p5) when the drill point enters into the seventh ply. In addition, it can be observed that thrust force of drilling with collars was higher than that of without plates. In combined drilling, the stiffness of the process system is increased because the deformation of the workpiece can be reduced by the supporting action of collars. Stiffness of the process system k can be calculated by $k = F_Z/Z$, where F_Z is the thrust force and Z is the corresponding displacement. Therefore, at the same displacement, the required thrust force will increase with the increase in stiffness of the process system.

Figure 13b–d shows the influence of inner diameter of collars on the distribution of the maximum thrust force at different feed speeds. As shown in Fig. 13b, during drilling with collars of 6.7 and 6.5 mm, thrust forces reach the maximum values of 43.7 N (point p13) and 49.5 N (point p10),

Table 3 Experimental results of delamination, tearing, and fuzzing defects during drilling of KFRP composites

Working condition	Size of collar c(mm)	Feed speed f (mm/min)								
		20			40			80		
		F_d	T	A_f (mm)	F_d	T	A_f (mm)	F_d	T	A_f (mm)
A_1	Without	1.408	1	33.50	1.433	1	27.63	1.450	1	14.69
A_2	6.1	1.037	0.473	9.00	1.047	0.526	14.04	1.083	0.549	14.29
A_3	6.3	1.080	0.550	9.04	1.077	0.647	14.94	1.100	0.668	16.04
A_4	6.5	1.100	0.664	11.13	1.133	0.745	16.02	1.147	0.783	16.53
A_5	6.7	1.117	0.719	25.37	1.143	0.773	18.35	1.167	0.813	14.91

respectively, when the drill point enters into the eighth ply. For the case with collars of 6.3 and 6.1 mm, thrust forces reach the maximum of 53.2 N (point p7) and 58.0 N (point p4), respectively, when the drill point enters into the seventh ply. It can be concluded that the supporting action of collars rises when inner diameter of collars varies from 6.7 to 6.1 mm, and the supporting action of collars has a positive effect on thrust force. Due to the low transition temperature and low thermal conduction of KFRP composites, the matrix will be softened by heat generated around cutting edge. Therefore, the heat generated increases with the increase of thrust force. In addition, the softened matrix serves as a lubricant material and reduces the friction forces and the moment of friction force on the margins [25]. Therefore, with the decrease in collar inner diameter from 6.7 to 6.1 mm, the position of the maximum thrust force moves toward the ply at which the whole main cutting edge enters into the laminate. The same phenomenon can be observed in Fig. 13c, d.

Figure 14 illustrates the positions of the drill point when thrust force reaches the maximum value in different working conditions. Since the trends at different feed speeds are the same, the result of $f = 80$ mm/min is discussed as an example. During drilling with collars of 6.1 and 6.3 mm, there were five uncut plies under the drill point when thrust forces reached the maximum values while with collars of 6.5 and 6.7 mm, there were four uncut plies under the drill point. During drilling without plates, only two uncut plies were left over when thrust forces reached the maximum value. Compared with working condition A_1, numbers of uncut plies increased by one ply in $f = 20$ mm/min, three plies in $f = 40$ mm/min, and three plies in $f = 80$ mm/min when the thrust forces reached the maximum value for working condition A_2.

Therefore, in the drilling process of KFRP composites, distribution of the maximum thrust force is closely related to feed speed and inner diameter of collars. During drilling without plates, the position of the maximum thrust force moves toward the exit when feed speed rises. This phenomenon can cause a high thrust force of the last layer. Furthermore, due to the decrease in the uncut thickness, the resistance to deformation declines rapidly. Therefore, the superimposed factors of high thrust force and low bending resistance result in severe delamination defect at the exit. In combined drilling, while the required thrust force increases with the rise of stiffness of the process system, the position of the maximum thrust force moves toward the ply of the whole main cutting edge entering into the laminate. The major consequences can be summarized as follows. Firstly, the thrust force during drilling the last ply is in a relatively low level. Secondly, bending resistance increases with the increasing thickness of the uncut lamina when thrust force reaches the maximum value. Therefore, the distribution of maximum thrust force in combined drilling is more appropriate than drilling without plates, such that defects at the exit can be reduced effectively.

5 Results and discussion

5.1 Characterization of hole quality

In this section, three characteristic indexes are introduced to evaluate the hole quality during drilling of KFRP composites. Delamination factor, tearing length ratio, and fuzzing area will be used to characterize delamination, tearing, and fuzzing defects, respectively. As shown in Fig. 15a, delamination factor F_d was defined as the quotient between the maximum diameter D_{MAX} of the delaminated area and the hole nominal diameter D. F_d can be calculated by Eq. 11 [27]. Since there is obvious color variation in the delaminated area of KFRP composites at the exit, the edge of delaminated area can be identified by visual inspection. Values of the maximum delaminated diameter were measured with a caliper.

$$F_d = D_{MAX}/D \tag{11}$$

As illustrated in Fig. 15b, tearing length ratio T was defined as the quotient between the arc length l of the tearing defect along the periphery of the hole and the nominal perimeter of hole (C). It can be calculated by Eq. 12. Digital images at the exit were tackled with AutoCAD software to measure the arc length.

$$T = l/C \tag{12}$$

Approaches based on digital image analysis have been previously used to assess drilling-induced damage after machining of composite laminates [28, 29]. Since the shape of the fuzzing area is irregular and difficult to quantify, it can be obtained using image digitalization technique. In this study, digital images at the entrance were transformed to binary picture using Image-Pro Plus software, and from these, the area of fuzzing defect A_f can be measured correctly. A representative binary picture is shown in Fig. 15c. The experimental results of delamination, tearing, and fuzzing defects are illustrated in Table 3.

5.2 Influence of inner diameter of collars on hole quality

Influence of inner diameter of collars on delamination defect is shown in Fig. 16. As feed speed varied from 20 to 80 mm/min, delamination factor of combined drilling was significantly lower than drilling without plates. In the case of $f = 20$ mm/min, reductions of delamination factor using different collars are 26.3% for 6.1-mm inner diameter, 23.3% for 6.3 mm, 21.9% for 6.5 mm, and 20.7% for 6.7 mm. Furthermore, delamination factor declined when collar inner diameter decreased. This phenomenon can be explained by the delamination model in Sect. 4.1. The threshold of thrust force of the

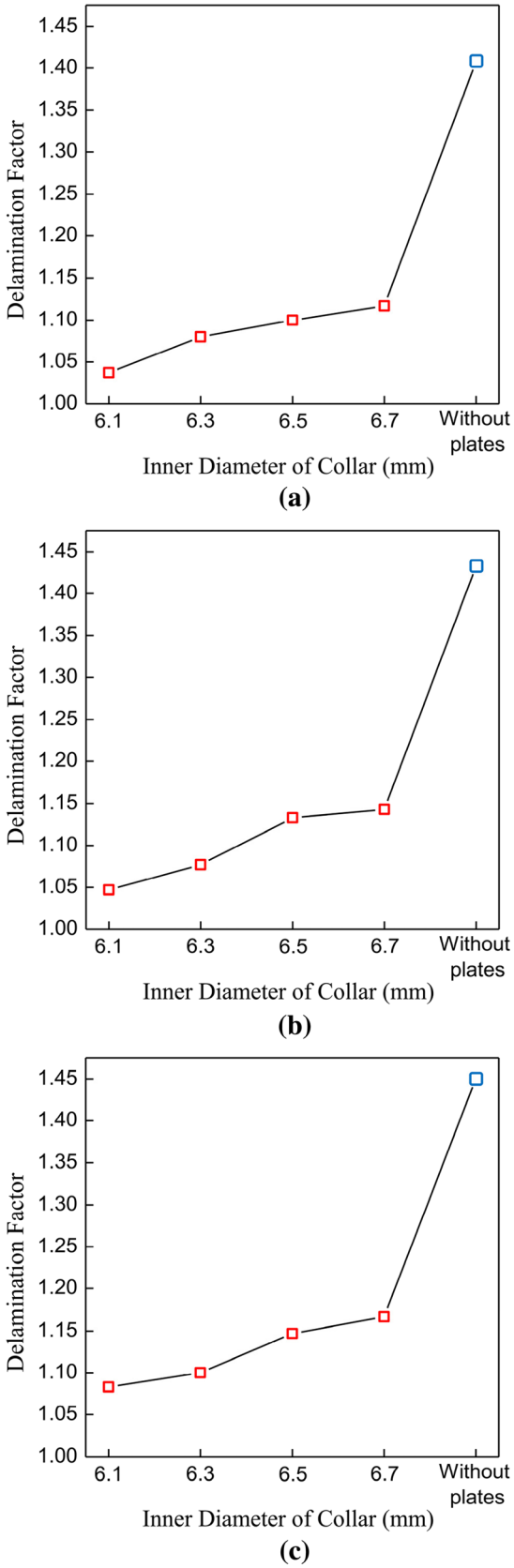

Fig. 16 Influence of inner diameter of collar on delamination defect. **a** f = 20 mm/min. **b** f = 40 mm/min. **c** f = 80 mm/min

onset of delamination rises with the decrease in collar inner diameter, such that the delamination can be less induced. Therefore, the effect of reducing delamination was improved.

In addition, the inner diameter of collars also had an important influence on tearing defect. As shown in Fig. 17, tearing length ratio of combined drilling is obviously lower than drilling without plates when feed speed increased from 20 to 80 mm/min. It can be observed that tearing length ratio rose with the increase in inner diameter of collars. Drilling with collars of 6.1 mm was the most effective, with a tearing length ratio of approximately 0.5. Smaller inner diameter of collars results in larger contact area between collars and material. Therefore, the supporting area and combined shearing action rise with the decrease in collar inner diameter, and the effect of reducing tearing defect was improved.

The influence of the inner diameter of collars on fuzzing defect is illustrated in Fig. 18. In the working condition of f = 20 mm/min, fuzzing area of drilling without plates was the highest, and reductions of fuzzing area using different collars are 73.1% for collar of 6.1 mm, 73.0% for collar of 6.3 mm, 66.8% for collar of 6.5 mm, and 24.3% for collar of 6.7 mm. Furthermore, the effect of reducing fuzzing defect was improved by decreasing inner diameter of collars. Likewise, smaller inner diameter of collars generates larger contact area between collars and material, such that the compressive area and combined shearing action rise by decreasing collar inner diameter. However, a different trend is observed in Fig. 18c. Fuzzing area rose first and then decreased when f = 80 mm/min. This phenomenon can be attributed to the influence of feed speed, and the detailed description is presented in the next section.

5.3 Influence of feed speed on hole quality

The influence of feed speed on delamination of working conditions A_1 and A_2 is shown in Fig. 19a. It can be seen that delamination factor rose with the increase in feed speed. These results are in agreement with the observations of drilling glass fiber-reinforced plastic (GFRP) and CFRP composites [12, 30]. When feed speed rises, the increase in cross-sectional area of the undeformed chip will result in the increase in resistance to deformation of the chip. Thrust force is the main cause of exit delamination. Therefore, the increase in thrust force aggravates exit delamination. In working condition A_2, the delaminated diameters were 0.22, 0.28, and 0.5 mm larger than the nominal diameter when feed speed increased from 20 to 80 mm/min. The growth of delamination diameter was acceptable. Hole quality at the exit of working conditions A_1 and A_2 is illustrated in Fig. 19b. It can be clearly observed that there were severe delamination defects at the exit during drilling without plates. In contrast, delamination defect in combined drilling was significantly reduced.

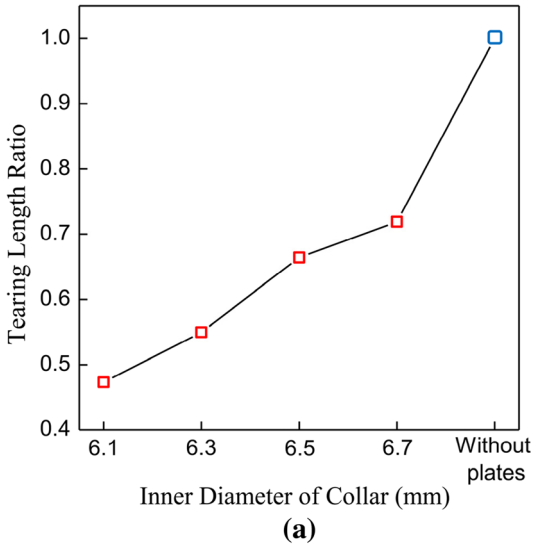

(a)

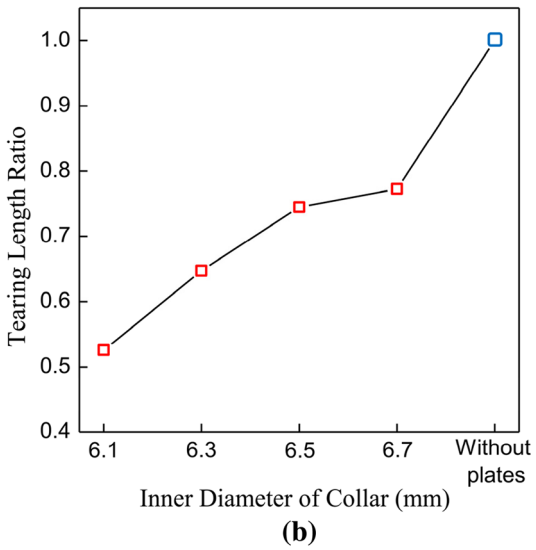

(b)

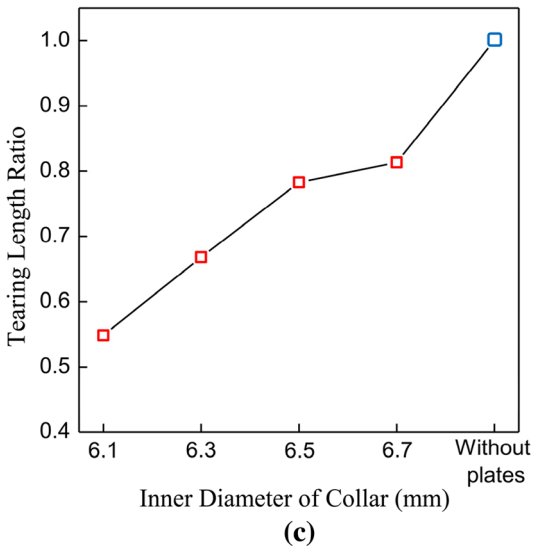

(c)

Fig. 17 Influence of inner diameter of collar on tearing defect. **a** f = 20 mm/min. **b** f = 40 mm/min. **c** f = 80 mm/min

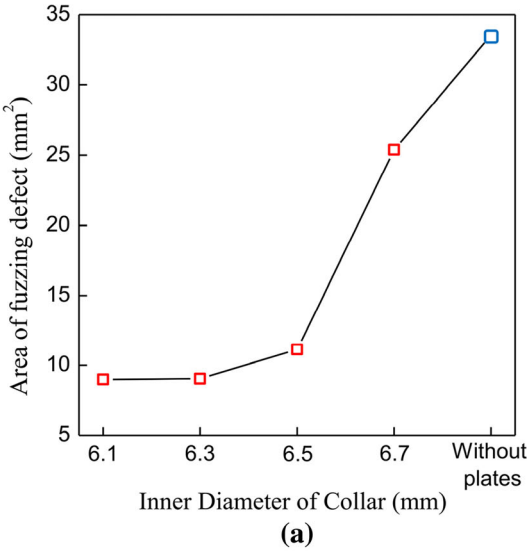

(a)

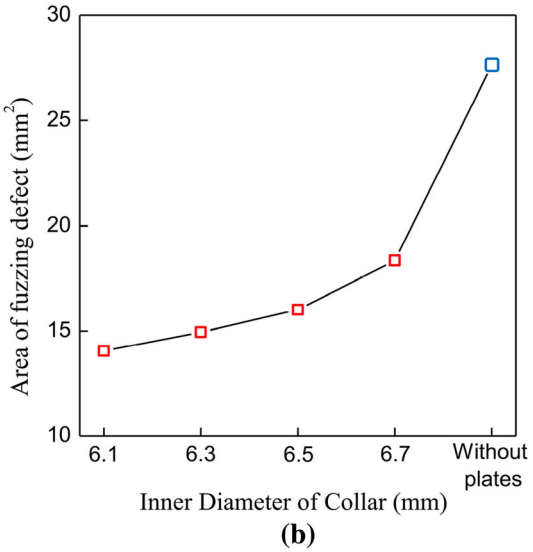

(b)

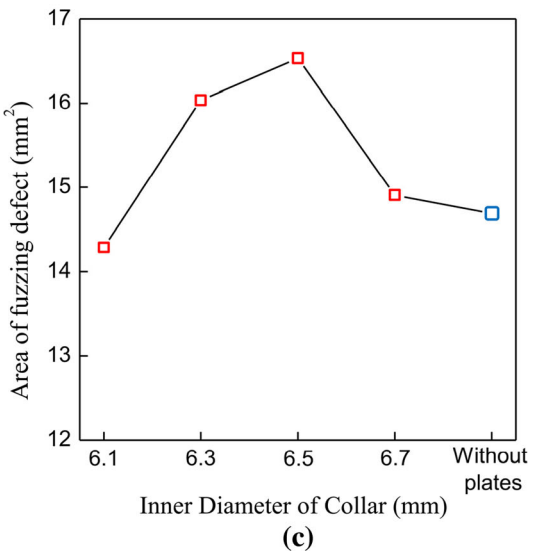

(c)

Fig. 18 Influence of inner diameter of collar on fuzzing defect. **a** f = 20 mm/min. **b** f = 40 mm/min. **c** f = 80 mm/min

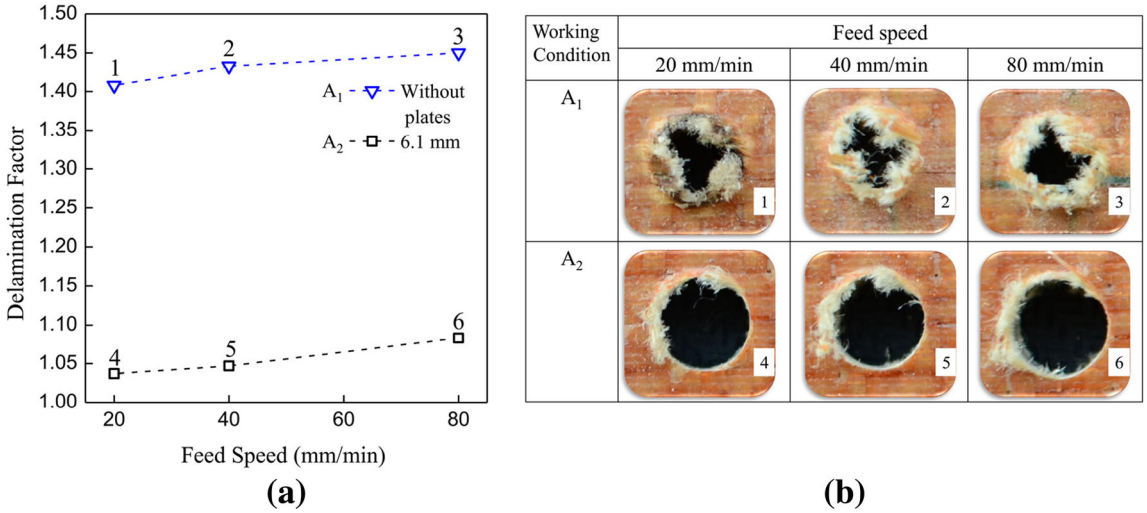

Fig. 19 **a** Influence of feed speed on delamination defect. **b** Hole quality at the exit

Figure 20 reveals the influence of feed speed on tearing defect of two working conditions. In working condition A_1, severe tearing defects occurred extensively. Thus, all of the tearing length ratios were 1.0. In contrast, the inhibitory effect on tearing defect was improved significantly in working condition A_2. Furthermore, tearing length ratio also rose by increasing feed speed. The conclusion agrees with the results of drilling CFRP composite [7]. Tearing defect is initiated by the punching action of the chisel edge. The punching action rises with the increase in feed speed. Therefore, the generation of tearing was aggravated. However, there was still residual tearing defect along one side of the circumference, and the other side was smooth. This phenomenon can be attributed to the inverted cone of the main cutting edge of the twist drill. Once the main cutting edge can no longer cut Kevlar fiber layers thoroughly within one spindle revolution, consecutive tearing defect will occur along the edge of the hole.

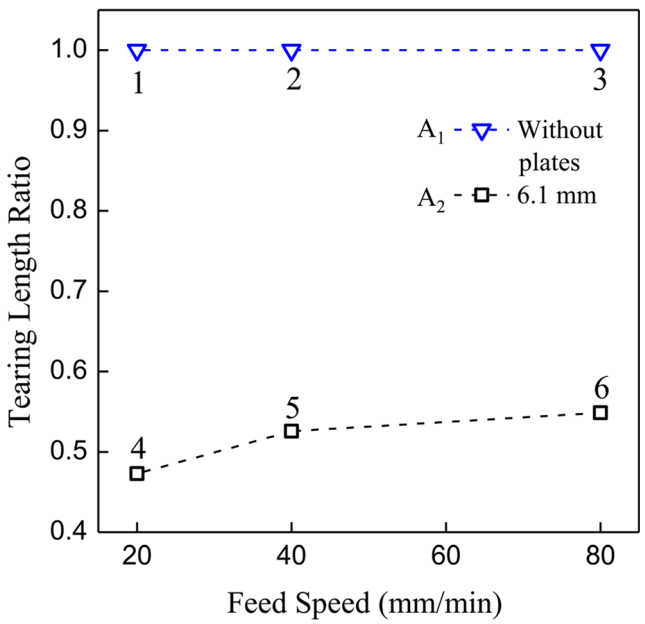

Fig. 20 Influence of feed speed on tearing defect

The influence of feed speed on fuzzing defect of working conditions A_1 and A_2 is shown in Fig. 21a. During drilling with collars of 6.1 mm, the area of fuzzing defect increased with the increase in feed speed, while still keeping a relatively low level. In contrast, the trend of drilling without plates was reverse: The area of fuzzing defect decreased. Since both fuzzing and entrance delamination are caused by peeling force at the entrance plane, we compare the results of fuzzing with those of entrance delamination of CFRP and GFRP. The conclusion disagrees with the results of entrance delamination by [12, 30]. The phenomenon can be explained by the mean chip thickness with different feed speeds. Due to the high toughness, few Kevlar fibers are cut by shear failure during drilling without plates. When feed speed rises, the mean chip thickness will be increased to strengthen the shearing action of the cutting edge [31, 32], and fuzzing defect will be reduced. Moreover, as shown in Table 3, fuzzing area also declined with the increase in feed speed using collar of 6.7 mm. It can be concluded that the influence of interaction between collars and cutter on fuzzing was weakened when inner diameter rose to 6.7 mm.

Hole quality at the entrance of working conditions A_1 and A_2 is shown in Fig. 21b. It can be observed that extensive and severe fuzzing defect covered along the hole edge at feed speeds of 20 and 40 mm/min without plates. Moreover, less severe but uneven fuzzing defect remained at $f = 80$ mm/min. In contrast, slight fuzzing defect was observed by using collar of 6.1 mm, and fuzzing defect was reduced significantly in combined drilling.

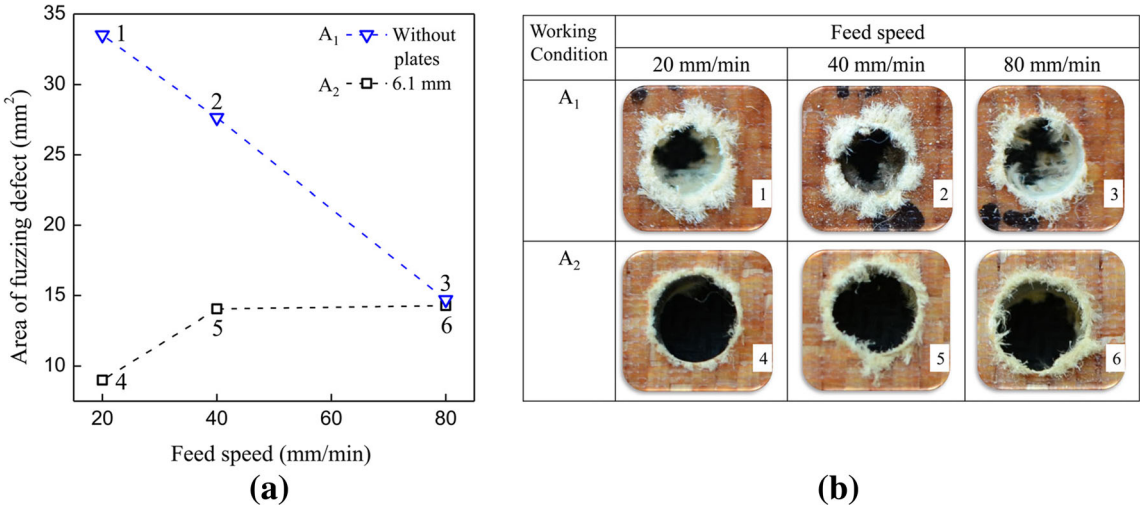

Fig. 21 **a** Influence of feed speed on fuzzing defect. **b** Hole quality at the entrance

6 Conclusions

This paper is focused on revealing the mechanisms of drilling-induced defects of KFRP composite (delamination, tearing, and fuzzing) through a systematic investigation. On this basis, a new approach (combined drilling) based on the interaction between collars and cutter was presented to reduce damages. Drilling experiments were conducted to study the influence of collar inner diameter and feed rate on the thrust force and hole quality. From the analysis and experimental results, some conclusions can be drawn as follows:

1. Delamination occurs at some point when thrust force exceeds the interlaminar bonding strength. The low interfacial bonding between Kevlar fibers and the matrix can lead to more severe delamination. Tearing defect is initiated when the exit layer splits around the drill point under the punching action of the chisel edge. Tensile failure of the majority of fibers causes tearing defect along the edge of hole. Peeling action at the entrance plane results in obvious yield and necking of Kevlar fiber. Due to the high toughness, fibers fracture after plastic deformation to generate fuzzing defect.
2. During combined drilling, stiffness of the process system was increased to inhibit delamination propagation. The combined shearing action between cutting edge and the edge of the hole-wall of the collar strengthens shear fracture of Kevlar fibers at the exit and entrance planes of the laminate. The experimental results showed that machining defects can be reduced effectively.
3. A delamination model based on the interaction between collars and cutter was proposed to predict the critical thrust force for the onset of delamination. Moreover, distribution of the maximum thrust force is closely related to feed speed and support configurations. In combined drilling, the position of the maximum thrust force moves toward the ply of the whole main cutting edge entering into the laminate, which is more appropriate than drilling without plates.
4. A process guidance was provided to optimize the hole quality during drilling of KFRP composite. The optimal drilling parameters are collar of 6.1 mm and feed speed of 20 mm/min. Compared to drilling without collars, reductions of defects are 26.3% for delamination factor, 52.7% for tearing length ratio, and 73.1% for fuzzing area.

Funding information This work is supported by the National Natural Science Foundation of China (Grant No. 11372220).

References

1. Abhishek K, Datta S, Mahapatra SS (2015) Optimization of thrust, torque, entry, and exist delamination factor during drilling of CFRP composites. Int J Adv Manuf Technol 76(1–4):401–416. https://doi.org/10.1007/s00170-014-6199-3
2. Soutis C (2005) Fibre reinforced composites in aircraft construction. Prog Aerosp Sci 41(2):143–151. https://doi.org/10.1016/j.paerosci.2005.02.004
3. Bhattacharyya D, Horrigan DPW (1998) A study of hole drilling in Kevlar composites. Compos Sci Technol 58(2):267–283. https://doi.org/10.1016/S0266-3538(97)00127-9
4. Shuaib AN, Al-Sulaiman FA, Hamid F (2004) Machinability of Kevlar® 49 composite laminates while using standard TiN coated HSS drills. Mach Sci Technol 8(3):449–467. https://doi.org/10.1081/MST-200041116
5. Persson E, Eriksson I, Zackrisson L (1997) Effects of hole machining defects on strength and fatigue life of composite laminates. Compos Part A Appl Sci Manuf 28(2):141–151. https://doi.org/10.1016/S1359-835X(96)00106-6
6. König W, Graß P (1989) Quality definition and assessment in drilling of fibre reinforced thermosets. CIRP Ann-Manuf Technol 38(1):119–124. https://doi.org/10.1016/S0007-8506(07)62665-1

7. Wang GD, Li N, Xiong XH, Chong Q, Zhou L, Lu SW (2017) 3D level comprehensive evaluation of hole quality in drilling carbon fiber-reinforced plastics. Int J Adv Manuf Technol 93(5-8):2433–2445. https://doi.org/10.1007/s00170-017-0614-5
8. Ho-Cheng H, Dharan CKH (1990) Delamination during drilling in composite laminates. J Eng Ind 112(3):236–239. https://doi.org/10.1115/1.2899580
9. Liu D, Tang Y, Cong WL (2012) A review of mechanical drilling for composite laminates. Compos Struct 94(4):1265–1279. https://doi.org/10.1016/j.compstruct.2011.11.024
10. Capello E (2004) Workpiece damping and its effect on delamination damage in drilling thin composite laminates. J Mater Process Technol 148(2):186–195. https://doi.org/10.1016/S0924-0136(03)00812-4
11. Zhang HJ, Chen WY, Chen DC, Zhang LC (2001) Assessment of the exit defects in carbon fibre-reinforced plastic plates caused by drilling. Key Eng Mater 196(8):43–52. https://doi.org/10.4028/www.scientific.net/KEM.196.43
12. Davim JP, Reis P (2003) Drilling carbon fiber reinforced plastics manufactured by autoclave—experimental and statistical study. Mater Des 24(5):315–324. https://doi.org/10.1016/S0261-3069(03)00062-1
13. Kim SC, Kim JS, Yoon HJ (2011) Experimental and numerical investigations of mode I delamination behaviors of woven fabric composites with carbon, Kevlar and their hybrid fibers. Int J Precis Eng Man 12(2):321–329
14. Wan YZ, Chen GC, Huang Y, Li QY, Zhou FG, Xin JY, Wang YL (2005) Characterization of three-dimensional braided carbon/Kevlar hybrid composites for orthopedic usage. Mater Sci Eng A 398(1–2):227–232. https://doi.org/10.1016/j.msea.2005.03.010
15. Bunsell AR (1975) The tensile and fatigue behaviour of Kevlar-49 (PRD-49) fibre. J Mater Sci 10(8):1300–1308. https://doi.org/10.1007/BF00540819
16. Won MS, Dharan CKH (2002) Drilling of aramid and carbon fiber polymer composites. J Manuf Sci Eng 124(4):778–783. https://doi.org/10.1115/1.1505854
17. Gaitonde VN, Karnik SR, Rubio JC, Correia AE, Abrão AM, Davim JP (2008) Analysis of parametric influence on delamination in high-speed drilling of carbon fiber reinforced plastic composites. J Mater Process Technol 203(1-3):431–438. https://doi.org/10.1016/j.jmatprotec.2007.10.050
18. Davim JP, Reis P (2003) Study of delamination in drilling carbon fiber reinforced plastics (CFRP) using design experiments. Compos Struct 59(4):481–487. https://doi.org/10.1016/S0263-8223(02)00257-X
19. Abrão AM, Faria PE, Rubio JC, Reis P, Davim JP (2007) Drilling of fiber reinforced plastics: a review. J Mater Process Technol 186(1–3):1–7. https://doi.org/10.1016/j.jmatprotec.2006.11.146
20. Singh I, Bhatnagar N (2006) Drilling of uni-directional glass fiber reinforced plastic (UD-GFRP) composite laminates. Int J Adv Manuf Technol 27(9-10):870–876. https://doi.org/10.1007/s00170-004-2280-7
21. Tsao CC, Hocheng H (2005) Effects of exit back-up on delamination in drilling composite materials using a saw drill and a core drill. Int J Mach Tool Manu 45(11):1261–1270. https://doi.org/10.1016/j.ijmachtools.2005.01.015
22. Wern CW, Ramulu M, Shukla A (1996) Investigation of stresses in the orthogonal cutting of fiber-reinforced plastics. Exp Mech 36(1):33–41. https://doi.org/10.1007/BF02328695
23. Khashaba UA, El-Sonbaty IA, Selmy AI, Megahed AA (2010) Machinability analysis in drilling woven GFR/epoxy composites: part I—effect of machining parameters. Compos Part A Appl Sci Manuf 41(3):391–400. https://doi.org/10.1016/j.compositesa.2009.11.006
24. Nagao T, Hatamura Y (1988) Investigation into drilling laminated printed circuit board using a torque-thrust-temperature sensor. CIRP Ann-Manuf Technol 37(1):79–82. https://doi.org/10.1016/S0007-8506(07)61590-X
25. Khashaba UA, El-Keran AA (2017) Drilling analysis of thin woven glass-fiber reinforced epoxy composites. J Mater Process Technol 249:415–425. https://doi.org/10.1016/j.jmatprotec.2017.06.011
26. Dipaolo G, Kappor SG, Devor RE (1996) An experimental investigation of the crack growth phenomenon for drilling of fiber-reinforced composite materials. J Eng Ind 118(1):104–110. https://doi.org/10.1115/1.2803629
27. Chen WC (1997) Some experimental investigations in the drilling of carbon fiber-reinforced plastic (CFRP) composite laminates. Int J Mach Tool Manu 37(8):1097–1108. https://doi.org/10.1016/S0890-6955(96)00095-8
28. Davim JP, Rubio JC, Abrao AM (2007) A novel approach based on digital image analysis to evaluate the delamination factor after drilling composite laminates. Compos Sci Technol 67(9):1939–1945. https://doi.org/10.1016/j.compscitech.2006.10.009
29. Silva D, Teixeira JP, Machado CM (2014) Methodology analysis for evaluation of drilling-induced damage in composites. Int J Adv Manuf Technol 71(9-12):1919–1928. https://doi.org/10.1007/s00170-014-5616-y
30. Khashaba UA, El-Sonbaty IA, Selmy AI, Megahed AA (2010) Machinability analysis in drilling woven GFR/epoxy composites: part II—effect of drill wear. Compos Part A Appl Sci Manuf 41(9):1130–1137. https://doi.org/10.1016/j.compositesa.2010.04.011
31. Chegdani F, Mezghani S, Mansori ME (2015) Experimental study of coated tools effects in dry cutting of natural fiber reinforced plastics. Surf Coat Technol 284:264–272
32. Liu C, Wang GF, Ren CZ, Yang YW (2014) Mechanistic modeling of oblique cutting considering fracture toughness and thermo-mechanical properties. Int J Adv Manuf Technol 74(9-12):1459–1468. https://doi.org/10.1007/s00170-014-6100-4